Journal of Mechanical Design. Received February 07, 2018;
Accepted manuscript posted June 11, 2019. doi:10.1115/1.4044107

Design of a prototype for the in situ forming of a liquid infused preform (ISFLIP) process

Jaime Juan
Department of Materials Science and Metallurgy
Barcelona Tech
Terrassa 08034, Spain
jaime.juan@upc.edu

M. Núria Salán[1]
Department of Materials Science and Metallurgy
Barcelona Tech
Terrassa 08034, Spain
nuria.salan@upc.edu

Arlindo Silva
International Design Center
Engineering Product Development
Singapore University of Technology and Design
Singapore 487372
arlindo_silva@sutd.edu.sg
ASME Membership 102035333

José A. Tornero
Institute of Textile Research and Industrial Cooperation
Barcelona Tech
Terrassa 08034, Spain
jose.antonio.tornero@upc.edu

[1] Corresponding author.

ABSTRACT

The world is changing and demanding stronger, lighter and more versatile materials. Taking advantage of the full potential of these materials also requires versatile manufacturing processes. The in situ forming of a liquid infused preform (ISFLIP) is a new manufacturing process for fiber reinforced polymer (FRP) parts with shell shapes. ISFLIP is a hybrid process between vacuum infusion (VI) and diaphragm forming. This paper focuses on the mechanical design and experimental validation of a functional prototype of ISFLIP. The novelty of the design lies especially in a double diaphragm system that is fundamental to carrying out the forming just after the infusion stage. The double diaphragm system and other two major subsystems, a vacuum table and an infrared heating grid, were devised to benefit from the operational advantages of ISFLIP. The whole prototype, once constructed, was tested by forming some demonstration components. The result of one of these components, a 'C' cross-section FRP profile with two sharp joggles, is finally obtained, proving the feasibility of the prototype.

Keywords: functional prototype, mechanical design, design validation, manufacturing, composite materials

1 INTRODUCTION

Even in competitive industries such as aviation and automotive, fiber reinforced polymers (FRP) have experienced continuous growth in the last decade and show promising prospects [1]. The main reasons for this growth are the impressive specific mechanical properties of FRPs and the increasing need for lightweight materials [2,3]. Clear examples of this recent trend are the Airbus A350 XWB and the Boeing 787 Dreamliner in aviation, and the BMW i3 in automotive. However, FRPs still present some manufacturing barriers to achieve large, economic batch sizes while keeping high quality standards, and without compromising the scalability and flexibility associated with FRPs [4,5].

Liquid composite molding (LCM) techniques show great potential for overcoming traditional production limitations associated with FRPs. LCM covers techniques in which a polymeric resin in liquid state (matrix) impregnates a textile preform (reinforcement). A “textile preform”, or just “preform”, is an arrangement of textile reinforcements that has been formed into a shape which closely resembles the final part. The resin impregnates the preform due to the action of a positive pressure difference between a resin deposit and the cavity which contains the preform.

LCM techniques may be split into two categories according to the nature of the driving pressure: resin transfer molding (RTM), in which resin is pumped into the preform cavity under pressure; and vacuum infusion (VI), in which vacuum pressure is applied into the preform cavity to pull the resin into the preform.

In previous work, we proposed a new VI variant: the in situ forming of a liquid infused preform (ISFLIP) [6,7]. ISFLIP is a hybrid process between VI and diaphragm forming. This new process was conceived as a real alternative to manufacturing high performance FRP parts with shorter processing times and higher reproducibility than other conventional VI techniques.

As a first stage of ISFLIP development, in this paper, it has been addressed the design of a functional prototype which is expected to allow for a future validation of ISFLIP. A series of design requirements were defined according to the operational advantages that ISFLIP offers. From these requirements, the key design aspects of the major mechanical subsystems of the prototype are provided. Finally, it is provided an

Journal of Mechanical Design. Received February 07, 2018;
Accepted manuscript posted June 11, 2019. doi:10.1115/1.4044107

insight into the experimental procedure carried out to proof the prototype feasibility for manufacturing a FRP parts via ISFLIP.

.

2 ISFLIP OVERVIEW

A basic flowchart of ISFLIP is depicted in Fig. 1. In ISFLIP, a flat preform consisting of a stack of reinforcement fabrics is first impregnated with a low viscosity resin. Then, the impregnated preform is formed over a mold while the resin is still in the low viscosity state. Finally, the matrix polymerizes to yield the FRP component. In FRP manufacturing, this last step is usually conducted at a higher-than-ambient temperature to accelerate the polymerization reaction.

In conventional LCM techniques, any forming step is carried out before preform impregnation. However, the processing sequence followed in ISFLIP is possible because the preform assembly is clamped between two elastic diaphragms. These diaphragms keep the preform flat during the infusion stage and allow its subsequent vacuum forming.

This manufacturing sequence is shared with other hybrid VI-forming manufacturing techniques such as the Flexible Resin Transfer Molding (FRTM) [8] and the Resin Infusion between Double Flexible Tooling (RIDFT) [9,10]. In FRTM, separate sheets of solid resin and dry fiber fabrics are placed together between the two elastomeric diaphragms and heated to liquefy the resin; while in ISFLIP and RIDFT, a low viscosity resin is pulled from an external container.

Journal of Mechanical Design. Received February 07, 2018;
Accepted manuscript posted June 11, 2019. doi:10.1115/1.4044107

Unlike these other VI-forming variants [8,9], not only the preform is formed in a stand-alone process. Actually, a whole preform assembly (preform and auxiliary materials which are hermetically sealed by bagging films) is formed. Therefore, there are three air-tight cavities in ISFLIP: between the lower diaphragm and a vacuum table, between both diaphragms and inside bagging films. Although adding complexity to the system, this additional cavity with respect to RIDFT allows for a more secure impregnation of the preform, and gives more margin to adjust inlet and venting pressures to maximize part quality (maximize fiber volume fraction and minimize part porosity).

Auxiliary materials formed together with the preform allow for conducting and accelerating the impregnation of the preform, and to unmold the part once the resin is cured without any laborious preparation of the diaphragms. Prediction of the filling flow is considerably facilitated in ISFLIP because of the impregnation of a flat preform instead of a fully developed three-dimensional shape.

It is worth noting that elastic diaphragms used in ISFLIP are not supposed to include any embedded heating system. This approach is usually followed in the literature when trying to shorten resin curing time [11,12]. However, this might well increase the rigidity of diaphragms and reduce their maximum elongation.

Placement of reinforcement fabrics onto molds is a significant source of variability in FRP parts [13] and a very time-consuming and, thus, expensive task [14,15]. Conducting an automated forming step helps to reduce both drawbacks since the forming process starts from a flat preform. Gains in reproducibility and savings in time consumption increase as the shape complexity increases. Nevertheless, as shape complexity increases, successfully forming the preform in a single step is also more difficult. Furthermore, preforming automation in the case of stacks of two-dimensional fabrics is mostly limited to flat or almost flat preform geometries [14,16].

ISFLIP is appropriate for all kinds of preforms based on stacks of two-dimensional fabrics, and it targets shell shape components. Simple shapes (flat or single curvature) to more complex double curvature shapes may be obtained. In order to be formable, shells should be non-reentrant and, in the case of double curvature shapes, also shallow:

- Automotive parts such as ‘B’ pillars, transmission tunnels or leaf springs.
- Shells of wind turbine blades.
- ‘L’, ‘C’ or ‘U’ cross-section composite beams (straight, single curved and double curved).

Furthermore, ISFLIP has great potential in terms of production volume. Preform stacking and impregnation can be conducted without the need of molds. Therefore, in-mold cycle time is limited to the forming, curing and unmolding steps. Short cycle times (< 30 min) may be reached depending on the part size and shape and the resin system. This considerable reduction in in-mold cycle time with respect to conventional VI-like techniques, in combination with a part size range which cannot be reached by RTM-like techniques (ISFLIP part size range between 0.1 – 50 m^2), would allow ISFLIP to fill a market niche not covered in the current FRP industry.

3 DESIGN REQUIREMENTS

Journal of Mechanical Design. Received February 07, 2018;
Accepted manuscript posted June 11, 2019. doi:10.1115/1.4044107

The requirements which guided the design of the prototype are listed in Table 1. Requirements were defined according to previous experience in similar production systems, such as vacuum forming, and the operational advantages of ISFLIP introduced in the previous section. Design requirements were expressed as functions, constraints and objectives [17].

Table 1. Design requirements for the ISFLIP prototype.

Code	Requirement	Motivation
Functions		
Func1	Able to manufacture a variety of representative FRP components.	Keeping always the focus on the ultimate quality attribute which is the FRP part.
Func2	Two independent air-tight cavities able to fully evacuate air inside.	Taking advantage of ISFLIP potential to reduce in-mold cycle time requires uncoupling forming and curing steps from preform preparation and infusion.
Func3	Secure impregnation of the preform.	Maximizing part quality inevitable requires ensuring a correct VI.
Func4	Secure control of the preform position all along the process.	In order to ensure fiber distribution accuracy and reproducibility into the manufactured part, both preform and mold positions should be controlled along the process.
Func5	Stable support of the mold.	
Func6	Accurate alignment between the vacuum table and the double diaphragm tooling.	
Constraints		
Cons1	Modular system.	Flexibility and versatility are key aspects in order for the prototype to adapt to different part typologies and manufacturing conditions.
Cons2	Diaphragms able to hold elastic deformation larger than 500%.	
Cons3	Working temperature above 120°C for elements subject to heating.	The prototype is expected to be able to work with polymeric matrices with cure temperature up to 120 °C.
Cons4	Heating power able to reach 120°C into the part.	
Objectives		
Obj1	As human powered as possible.	In order to keep cost under controlled.
Obj2	To facilitate manual operations*.	One of the advantages of ISFLIP is the reduction of part quality dependence on labor skills. However, some steps still require technician's participation, and these should be kept simple.
Obj3	Minimum interference with the preparation of the preform assembly.	
Obj4	Minimum cost.	The prototype was design under the principles of simplicity, safety and cost control.
Obj5	Maximum simplicity.	
Obj6	Maximum reliability	

*Any task that might not well be automated in a future production machine should be carried out by operators quickly and comfortably.

Journal of Mechanical Design. Received February 07, 2018;
Accepted manuscript posted June 11, 2019. doi:10.1115/1.4044107

4 PROTOTYPE DESIGN

This section focuses on three major subsystems: the double diaphragm tooling, the vacuum table, and the heating grid. Figure 2 shows the modular assembly of the system (fulfillment of Cons1). The novelty of the design lies in these three main subsystems, especially in the double diaphragm tooling.

The prototype is intended for the manufacture of FRP components with an elongated shell shape. The maximum size of the manufactured FRP components is given by the effective work area of the vacuum table, which is 1970 x 970 mm. These dimensions are enough to enable the manufacture of small FRP parts representative of real applications, such as those listed in Section 2 (Func1). Only aluminum structural elements are used in the prototype to reduce its total weight and make it manually operable (Obj1).

4.1 Double diaphragm tooling

The double diaphragm tooling (A) is split in three frames (Fig. 3.a). The lower and upper frames (A1 and A3) hold the elastic diaphragms. These frames are based on an extruded, T-slotted aluminum profile system. Profiles are bolted to each other and silicone hoses are pressurized into the slots of the profiles to hold the diaphragms (Fig. 3.b). This clamping system allows for fast and secure attachment of the diaphragms (Obj2).

The most usual materials for elastic diaphragms are latex and silicone, but only silicone offers a service temperature above 120℃ (Cons3). Therefore, silicone sheets of 1 mm thickness are used. This thickness is a good compromise between tear resistance

(Obj6) and small bending radii in concave shapes (Func1). With this sheet thickness, less than 20 mm radii in concave shapes are not expected to be reached. The silicone sheets show elastic deformations over 500% (Cons2) and are translucent. Translucent diaphragms allow for visual inspection of preform filling (Func3) and visual control of the position of the preform between the diaphragms (Func4).

Diaphragms are mounted on the lower and upper frames (A1 and A3) without any pre-stretching. Mounting pre-stretched diaphragms is very laborious. Figure 3.b depicts one of the frames with a loose diaphragm, since the diaphragms are initially simply held and not tightened. Figure 3.c shows how the diaphragm tightens once the lower frame (A1) is coupled to the central frame (A2). A loose diaphragm could result in undesired movements of the preform or even distortions. Therefore, the adopted configuration with three rigid frames ensures a tight clamp of the preform assembly (Func4). The lower and upper frames (A1 and A3) are coupled to the central frame (A2) by a series of strap clamps (eye bolt, wing screw and 'U' clamp) placed along the perimeter (Fig. 3.d).

Bending of lower and upper diaphragms over the interior plate of the central frame (A2) creates a clear and reliable double sealing contour (Obj6). Both contours form the airtight cavity containing the preform assembly (Func2). For brevity, hereinafter, the airtight cavity between both elastic diaphragms will be referred as "diaphragms cavity".

Figure 3.d shows a cross-section view of the diaphragms cavity after air evacuation. This configuration simplifies and minimizes the number of welding joints

Journal of Mechanical Design. Received February 07, 2018;
Accepted manuscript posted June 11, 2019. doi:10.1115/1.4044107

and does not require the use of sealants (Obj4 and Obj5). Welding is reduced to the central frame (A2) in which straight sections of the interior plate were welded to bent sections to create a hermetic frame. Round corners protect diaphragms from tearing (Obj6).

Furthermore, the central frame (A2) was reinforced with 'U' cross-section profiles to resist loads exerted by the pressure difference between the interior and exterior of the diaphragms cavity (Obj6). Applied loads could lead to considerable bending deformation. When both the lower and upper frames (A1 and A3) are coupled to the central frame (A2), two aluminum plates are mounted to share the loads between all three frames (Fig. 3.d).

The selected configuration of three rigid frames, and the easy attachment and detachment of the diaphragms, considerably facilitate the stacking of the preform and the set-up of the preform assembly (Obj2 and Obj3). For this purpose, pass-through connectors are also mounted in the central frame (A2). These connectors are intended to provide an airtight crossing path into the diaphragms cavity for the inlet and venting channels of the preform assembly. This option was preferred instead of passing through the elastic diaphragms for two reasons: the preparation of the preform assembly is more comfortable for the operators (Obj2); and the reliability of the system is increased (Obj6). Since diaphragms are held to high deformation levels during the forming stage, a hole in the diaphragm is a potential point of failure.

Journal of Mechanical Design. Received February 07, 2018;
Accepted manuscript posted June 11, 2019. doi:10.1115/1.4044107

The total weight of the double diaphragm tooling is approximately 50 kg (Obj1). Therefore, it can be managed by two operators throughout the different stages of ISFLIP.

4.2 Vacuum Table

The main function of the vacuum table (B) is to support the mold (Func5) while allowing an effective air evacuation. For this purpose, a flat table configuration was chosen to minimize construction cost (Obj4) and keep the design as simple as possible (Obj5). All elements forming the vacuum table (B) are shown in Fig. 4.a.

The “mold cavity” is formed between the lower diaphragm and a non-perforated aluminum plate with a thickness of 5 mm. The lower diaphragm, pushed by the central frame (A2), sits on the aluminum plate through a rectangular silicone joint to ensure optimal sealing between both elements (Fig. 4.b). The combination of a perforated aluminum plate with a thickness of 2 mm and a riveted grid of aluminum profiles allows for the effective evacuation of air from any point (Func2).

The supporting structure of the vacuum table (B) also guides the coupling with the double diaphragm tooling (A) and serves to fasten both subsystems (Cons1). A number of polyamide guides are mounted on the lower frame (A1) to ensure accurate alignment between subsystems (Func6). A clearance of 2 ±1 mm was left between the polyamide guides and the supporting structure.

In a future production machine, the alignment between mold and preform may be carried out through laser pointers placed over the mold. In the present prototype, the alignment between both elements is carried out through visual reference marks

Journal of Mechanical Design. Received February 07, 2018;
Accepted manuscript posted June 11, 2019. doi:10.1115/1.4044107

placed on the preform assembly and the mold. Translucency of the diaphragms allows both marks to overlap (Func4).

It is worth noting that the size of unit cells of typical reinforcement fabrics used in structural applications is often greater than 5 mm. Therefore, the position error between the preform and mold should not significantly affect the final fiber distribution into the FRP parts.

When the double diaphragm tooling is coupled to the vacuum table, its supporting structure also absorbs the lateral loads exerted on the central frame and limits its bending deformation (Obj6). Applying this configuration would be very useful in the case of larger machines, in which the increase in size of the frames might lead to considerable bending deformation.

4.3 Heating grid

Infrared radiation was chosen as the heating system (C) to accelerate the polymerization of the resin. Eighteen Elstein FSR 650 panel heaters (650W power) are arranged in three rows (Fig. 2). Previous experience shows that this power is enough to guarantee part temperatures above 120℃ (Cons4).

Each row is adjustable in x and y directions and their orientation can be changed along the z axis (Fig. 5). Furthermore, the position of each panel into the row is also adjustable in y direction, although the total stroke is only 40 mm. This configuration of infrared heaters is very flexible (Func1). Infrared heaters are connected in pairs that might later be assigned to different heating sectors. During processing, a PID controller

Journal of Mechanical Design. Received February 07, 2018;
Accepted manuscript posted June 11, 2019. doi:10.1115/1.4044107

activates or deactivates each sector according to the temperature of the upper diaphragm (one temperature measure per heating sector).

Temperature homogeneity was not included as a design requirement because the ability to keep it under reasonable limits is beyond the hardware described in this section. Temperature homogeneity will specifically depend on the efficacy of the control system and the position of the heaters with respect to the part.

A temperature tolerance of ±3°C of the preset target value would be enough during the curing cycle of ISFLIP, provided that a later post-curing cycle is carried out in a separate oven. A post-curing step ensures that the resin reaches optimal properties.

5 PROTOTYPE BUILDING

A prototype was successfully built to evaluate the design described in the previous section (Fig. 6). The prototype includes, apart from the three major sub-systems, a removable enclosure based on medium density fiberboard panels with a thickness of 10 mm and a movable structure built from standard T-slotted aluminum profiles.

In order to conduct ISFLIP, some additional equipment is necessary: one vacuum pump to evacuate air from both airtight cavities of the prototype; and another vacuum pump and a vacuum chamber (volume 10 l) to conduct the infusion stage. Two rotary vane vacuum pumps (Becker U4.20) were chosen for this purpose. These sturdy and durable vacuum pumps have a maximum suction rate of 21 m^3/h and reach a maximum vacuum level of 0.15 kPa. The suction capacity of this vacuum pump model is enough to

Journal of Mechanical Design. Received February 07, 2018;
Accepted manuscript posted June 11, 2019. doi:10.1115/1.4044107

evacuate air from inside both airtight cavities in less than 1 min. Furthermore, the attainable vacuum level ensures that a high-quality infusion stage is conducted.

5.1 Tune-up of the elastic diaphragms

As a rubber-like material, silicone sheets exhibit a notable softening through the first loading cycles. After a few dozen cycles, the material reaches a permanent condition. This phenomenon is called the “Mullins effect” [18]. To compensate for this effect, up to 20 forming cycles were performed with only the base mold (Fig. 6) and then the diaphragms were re-attached to their respective frames.

5.2 Tune-up of the heating grid

For each new part geometry, a study of the view factors between the infrared heaters and the part is necessary to establish an initial configuration, position and orientation of the heaters [19,20]. Then, temperature variability must be verified over the corresponding mold (both diaphragms formed) with a thermographic camera.

6 EXPERIMENTAL VALIDATION

Experimental validation consisted of the fabrication of a series of representative FRP parts with the prototype following the ISFLIP manufacturing methodology (Fig. 1). The evaluation was addressed by ensuring that all design requirements collected in Table 1 were met in practice.

A total of eight specimens were manufactured, from hemisphere shape to different types of ‘C’ cross-section profiles, using either glass or carbon fiber reinforcements [7]. This section in particular provides insight into the manufacturing of one geometry benchmark that is representative of ISFLIP potential. That geometry benchmark was a convex 'C' cross-section profile of constant thickness and variable section dimensions.

6.1 Materials

The preform of reinforcements consisted of a stack of 9 layers of a carbon 2/2 twill-weave fabric (Angeloni GG 285 T2). As a matrix, an epoxy system (Sicomin SR 8100 – SD 8822) was used.

In ISFLIP, the auxiliary materials of the preform assembly play a key role in the formability of the preform due to their continuous interaction throughout the forming step. Although it is outside the scope of this paper to go into more detail on the configuration of a preform assembly for ISFLIP; it is worth making a couple of short remarks in this respect. (i) The double bagging film (upper and lower) is the main difference with respect to preform assemblies of conventional VI [21,22]. (ii) Auxiliary materials with expected high drapability or flexibility should be used.

6.2 Benchmark geometry

Since there is no direct contact between the part and the mold in ISFLIP, no special treatment of the mold surface is necessary. Furthermore, the elastic diaphragm works as a surface softener which opens the possibility of using modular molds.

Figure 7 shows the mold used to manufacture the 'C' variable cross-section profile. The mold consisted of a succession of 'C' cross-section slices placed over a base tool. Rectilinear cross-section and variable cross-section slices were combined to intersperse sharp joggles (pronounced changes in outer section dimensions to provide clearance for other potential components) with uniform cross-section regions.

Journal of Mechanical Design. Received February 07, 2018;
Accepted manuscript posted June 11, 2019. doi:10.1115/1.4044107

6.3 Manufacturing

6.3.1 Preform assembly preparation

Preform stacking and preform assembly preparation were carried out over one of the silicone diaphragms, which was later attached to the lower frame. Then, the diaphragm was tightened by coupling the lower and central frames. At this point, the preform assembly was marked with two reference points for later alignment with the mold. Additionally, the inlet and venting channels of the preform assembly were connected to the resin deposit and vacuum chamber through the connectors mounted in the central frame. Finally, the diaphragms cavity was closed and air was evacuated from inside to clamp the preform assembly between both diaphragms. The pressure level inside the diaphragms cavity was set to -90 kPa.

6.3.2 Infusion

The infusion stage of ISFLIP starts with the clamping of the inlet channel and the ventilation of the air from the preform assembly. This action compresses the preform to maximize the final fiber volume fraction of the part. In this case, the pressure level inside the preform assembly was set to -95 kPa (pressure at the vacuum chamber). After 30 min of preform compaction, the clamp of the inlet channel was removed to start the impregnation of the preform. The filling of the preform lasted for around 10 min (Fig. 8.a). The resin had been previously degassed. Once the preform was fully filled, the inlet channel was connected to the vacuum chamber and the pressure level set to -90 kPa, as well.

6.3.3 Forming

It is worth noting that up to this point the only subsystem involved in the process was the double diaphragm tooling. However, to proceed with the forming step, the double diaphragm tooling was placed over the vacuum table and both subsystems were partially fastened, leaving an opening between both elements. Through this opening, the mold could be aligned with respect to the preform assembly. The mold had been previously marked with two reference points that coincided with those of the preform assembly. Then, the mold cavity was closed and air was evacuated up to a pressure level of -90 kPa, forcing both diaphragms and the preform assembly to conform to the mold.

6.3.4 Curing

Immediately after finishing the forming step, the heating grid was fastened to the upper frame. Three thermocouples were placed over the upper diaphragm to control the three corresponding heating sectors (Fig. 8.b).The heating grid had been previously tuned-up to the geometry benchmark. The enclosure of the heating chamber was mounted and the curing step carried out. The curing step, defined to achieve a high degree of cross-linking of the resin, consisted of two consecutive periods of 60 min at 60°C and 120 min at 80°C (heating ramp of 3°C/min).

Once the system cooled down following completion of the curing step, the preform assembly was removed from the mold. To this end, the vacuum of the diaphragms cavity was released while vacuum suction in the mold cavity was still active to prevent any damage to the lower diaphragm. Finally, auxiliary materials of the preform assembly were separated from the 'C' variable cross-section profile.

6.4 'C' cross-section profile with joggles

The manufactured FRP profile is shown in Fig. 9. In forming of ‘C’ cross-section profiles with joggles, both intra-ply shear (trellis shear) [23] and ply-ply shear [24] were involved: intra-ply shear in joggle regions and ply-ply shear in bending over tight radii.

The required trellis shear for the preform to adapt to the joggle regions of the mold exceeded the deformation capacity of the reinforcement fabrics. Besides, this deformation capacity is even reduced when a normal pressure is exerted on the weave cross-overs [25,26] as occurs in ISFLIP, and in most automated forming attempts of multi-ply FRP components [27,28]. As a consequence, out-of-plane deformation happens and wrinkles appear in order for the whole stack to achieve a minimum energy state, as can be seen in Fig. 9.

Conversely, in rectilinear cross-section regions, where the main deformation mechanism was inter-ply shear, no wrinkles were formed. Under these conditions, slippage between layers was enough to accommodate the required translation despite the compaction pressure exerted by both diaphragms on the preform. It is worth emphasizing the positive effect of the resin (still in a low viscosity state) acting as a lubricant between the layers inside the preform assembly.

6.5 Evaluation

In Section 4, it is indicated how each requirement listed in Table 1 affected design decisions. However, requirements related to the operability of the prototype also had to be experimentally verified: all functional requirements (Func1 to Func6); and some objectives (Obj1 to Obj3, and Obj6). Those requirements defined as constraints

Journal of Mechanical Design. Received February 07, 2018;
Accepted manuscript posted June 11, 2019. doi:10.1115/1.4044107

and the rest of objectives (Obj4 and Obj5) were more related to design issues such as selection of components and design guidelines.

The functional requirements form a function structure whose elements coincide with the milestones of the manufacturing procedure described in the previous section. This function structure leads to the main goal of manufacturing a FRP part through ISFLIP, proof of fulfillment of which is the 'C' cross-section FRP profile shown in Fig. 9.

Furthermore, all other requirements related to the operability of the prototype (Obj1, Obj2 and Obj3) were also amply met. The prototype can be comfortably managed by two operators. Likewise, the double diaphragm tooling and the vacuum table were thoroughly devised to facilitate all manual operations of a future production machine; mainly, the stacking of the preform, the preparation of the preform assembly, and the final unmolding of the FRP part. Finally, no reliability issues arose during the test campaign as a sign of the prototype robustness (Obj6).

7 CONCLUSIONS

This paper has presented the mechanical design of a prototype intended for manufacturing FRP parts following the ISFLIP process, a hybrid process between VI and diaphragm forming.

The prototype is based on three major subsystems: the double diaphragm tooling, the vacuum table and the heating grid. The double diaphragm tooling and the vacuum table combine to create two hermetically sealed cavities: one cavity containing the preform to be infused and another containing the mold that gives the final shape to the part. The design of both cavities has much to do with the successful implementation

Journal of Mechanical Design. Received February 07, 2018;
Accepted manuscript posted June 11, 2019. doi:10.1115/1.4044107

of ISFLIP. Furthermore, the grid of infrared radiation heaters allows for the processing of polymeric matrices, which require a higher-than-ambient temperature to be cured or to accelerate the curing process.

The double diaphragm tooling is the most innovative point of the prototype. The adopted solution design enables an easy and fast attachment and detachment of the elastic diaphragms. Likewise, the system also allows the diaphragms to be tightened after being mounted, facilitating the mounting action. These features are important for managing expected and unexpected replacements of diaphragms during production and for ensuring that ISFLIP is carried out at high quality standards.

The solutions reached for both the double diaphragm tooling and the vacuum table allow for clear and well-defined sealing contours, as well as minimizing welded joints and the use of sealants. This was achieved despite the high level of accessibility required for both airtight cavities and without compromising process reliability. Moreover, the chosen solutions are easily scalable to larger prototypes or production machines.

The prototype was validated by successfully manufacturing a 'C' cross-section profile with two sharp joggles. This manufacturing test served to prove that the prototype meets the requirements established by ISFLIP and, hence, to prove the ISFLIP concept. Additionally, the chosen type of geometry is representative of the potential of ISFLIP to be applied in shell shape FRP components, with shallow geometries in case of double curvature shapes and being highly effective to bend single curvature sections.

The presented ‘C’ cross-section profile should be understood as the starting point for future ISFLIP development. This development will include further research to learn more about the mechanisms involved in the forming process, the appropriate selection of auxiliary materials to maximize ISFLIP formability, and the employment of more advanced forming strategies. The ultimate goal of all of this work is to implement ISFLIP in a real production environment with a fully equipped production machine.

ACKNOWLEDGMENTS

This work was funded by SENER Ingeniería y Sistemas and the School of Industrial, Aerospace and Audiovisual Engineering of Terrassa (ESEIAAT). The authors would like to thank all of the staff at COMPOLAB for their invaluable help and Víctor Morell for his continuous support.

REFERENCES

[1] Holmes, M., 2014, "Global Carbon Fibre Market Remains on Upward Trend," Reinf. Plast., **58**(6), pp. 38–45. DOI: 10.1016/S0034-3617(14)70251-6.

[2] Soutis, C., 2005, "Fibre Reinforced Composites in Aircraft Construction," Prog. Aerosp. Sci., **41**(2), pp. 143–151. DOI: 10.1016/j.paerosci.2005.02.004.

[3] Fuchs, E. R. H., Field, F. R., Roth, R., and Kirchain, R. E., 2008, "Strategic Materials Selection in the Automobile Body: Economic Opportunities for Polymer Composite Design," Compos. Sci. Technol., **68**(9), pp. 1989–2002. DOI: 10.1016/j.compscitech.2008.01.015.

[4] Bader, M. G., 2002, "Selection of Composite Materials and Manufacturing Routes for Cost-Effective Performance," Compos. Part A Appl. Sci. Manuf., **33**(7), pp. 913–934. DOI: 10.1016/S1359-835X(02)00044-1.

[5] Khan, L. A., and Mehmood, A. H., 2016, "Cost-Effective Composites Manufacturing Processes for Automotive Applications," *Lightweight Composite Structures in Transport*, J. Njuguna, ed., Woodhead Publishing, Cambridge, UK, pp. 93–119. DOI: 10.1016/B978-1-78242-325-6.00005-0.

[6] Juan, J., Salán, N., and Tornero, J. A., 2015, "Sistema Y Procedimiento de Infusión de Resina Por Vacío Para La Obtención de Piezas Elaboradas a Partir de Materiales Compuestos," Spanish Patent 2551180 B2.

[7]Juan, J., 2017, "Development of the In Situ Forming of a Liquid Infused Preform (ISFLIP) Process. A New Manufacturing Technique for High Performance Fibre Reinforced Polymer (FRP) Components," Ph.D thesis, Barcelona Tech, Terrassa, Spain.

[8] Foley, M. F., 1992, "The Flexible Resin Transfer Molding (FRTM) Process," SAMPE J., **28**, pp. 15–24.

[9] Thagard, J. R., Okoli, O. I., Liang, Z., Wang, H. P., and Zhang, C., 2003, "Resin Infusion between Double Flexible Tooling: Prototype Development," Compos. Part A Appl. Sci. Manuf., **34**(9), pp. 803–811. DOI: 10.1016/S1359-835X(03)00201-X.

[10] Zhang, K., Gu, Y., Zhang, J., Li, M., Wang, S., and Zhang, Z., 2015, "Rapid Curing Vacuum-Assisted Resin Infusion Molding Using Silicone Rubber Sheet Heater and the Effect of Cooling Process on the Properties of Carbon Fiber/Epoxy Composites," J. Compos. Mater., **50**(13), pp. 1837–1850. DOI: 10.1177/0021998315597990.

[11] Thagard, J. R., Okoli, O. I., and Liang, Z., 2004, "Resin Infusion between Double Flexible Tooling: Evaluation of Process Parameters," J. Reinf. Plast. Compos., **23**(16), pp.

1767–1778. DOI: 10.1177/0731684404041148.
[12] Fang, X., Bi, C., Hong, Y., Cho, K. H., Park, M. S., Wang, Y., and Yao, D., 2016, "Rapid Vacuum Infusion and Curing of Epoxy Composites with a Rubber-Cushioned Mold Design," Polym. Plast. Technol. Eng., **55**(10), pp. 1030–1038. DOI: 10.1080/03602559.2015.1132453.

[13] Mesogitis, T. S., Skordos, A. A., and Long, A. C., 2014, "Uncertainty in the Manufacturing of Fibrous Thermosetting Composites: A Review," Compos. Part A Appl. Sci. Manuf., **57**(0), pp. 67–75. DOI: 10.1016/j.compositesa.2013.11.004.

[14] Linke, M., Greb, C., Klingele, J., Schnabel, A., and Gries, T., 2012, "Automating Textile Preforming Technology for Mass Production of Fibre-Reinforced Polymer (FRP) Composites," *The Global Textile and Clothing Industry*, R. Shishoo, ed., Woodhead Publishing, Cambridge, UK, pp. 171–195. DOI: 10.1533/9780857095626.171.

[15] Elkington, M., Ward, C., Chatzimichali, A., and Potter, K., 2015, "Studying Effects of Preshearing on Hand Layup," Adv. Manuf. Polym. Compos. Sci., **1**(2), pp. 80–93. DOI: 10.1179/2055035914Y.0000000007.

[16] Belhaj, M., Deleglise, M., Comas-Cardona, S., Demouveau, H., Binetruy, C., Duval, C., and Figueiredo, P., 2013, "Dry Fiber Automated Placement of Carbon Fibrous Preforms," Compos. Part B Eng., **50**(0), pp. 107–111. DOI: 10.1016/j.compositesb.2013.01.014.

[17] Ashby, M., Shercliff, H., and Cebon, D., 2007, "Strategic Thinking: Matching Material to Design," *Materials: Engineering, Science, Processing and Design*, Butterworth-Heinemann, Oxford, UK, pp. 29–46. ISBN: 978-0-7506-8391-3.

[18] Diani, J., Fayolle, B., and Gilormini, P., 2009, "A Review on the Mullins Effect," Eur. Polym. J., **45**(3), pp. 601–612. DOI: 10.1016/j.eurpolymj.2008.11.017.

[19] Taherian, H., and Ramiar, A., 2005, "A Novel Technique for Radiation Shape Factor Calculation Using CAD Software," Numer. Heat Transf. Part B Fundam., **48**(4), pp. 387–403. DOI: 10.1016/j.matpr.2017.01.143.

[20] Gupta, M. K., Bumtariya, K. J., Shukla, H. A., Patel, P., and Khan, Z., 2017, "Methods for Evaluation of Radiation View Factor: A Review," Mater. Today Proc., **4**(2), pp. 1236–1243. DOI: 10.1016/j.matpr.2017.01.143.

[21] Govignon, Q., Bickerton, S., Morris, J., and Kelly, P. A., 2008, "Full Field Monitoring of the Resin Flow and Laminate Properties during the Resin Infusion Process," Compos. Part A Appl. Sci. Manuf., **39**(9), pp. 1412–1426. DOI: 10.1016/j.compositesa.2008.05.005.

[22] Govignon, Q., Kazmi, S. M. R., Hickey, C. M. D., and Bickerton, S., 2011, "Control of

Laminate Quality for Parts Manufactured Using the Resin Infusion Process," *ICCM18: 18th International Conference of Composite Materials*, Jeju Island, Korea.

[23] Cao, J., Akkerman, R., Boisse, P., Chen, J., Cheng, H. S., de Graaf, E. F., Gorczyca, J. L., Harrison, P., Hivet, G., Launay, J., Lee, W., Liu, L., Lomov, S. V, Long, A., de Luycker, E., Morestin, F., Padvoiskis, J., Peng, X. Q., Sherwood, J., Stoilova, T., Tao, X. M., Verpoest, I., Willems, A., Wiggers, J., Yu, T. X., and Zhu, B., 2008, "Characterization of Mechanical Behavior of Woven Fabrics: Experimental Methods and Benchmark Results," Compos. Part A Appl. Sci. Manuf., **39**(6), pp. 1037–1053. DOI: 10.1016/j.compositesa.2008.02.016.

[24] Sachs, U., Akkerman, R., Fetfatsidis, K., Vidal-Sallé, E., Schumacher, J., Ziegmann, G., Allaoui, S., Hivet, G., Maron, B., Vanclooster, K., and Lomov, S. V., 2014, "Characterization of the Dynamic Friction of Woven Fabrics: Experimental Methods and Benchmark Results," Compos. Part A Appl. Sci. Manuf., **67**, pp. 289–298. DOI: 10.1016/j.compositesa.2014.08.026.

[25] Lin, H., Long, A. C., Sherburn, M., and Clifford, M. J., 2008, "Modelling of Mechanical Behaviour for Woven Fabrics under Combined Loading," Int. J. Mater. Form., **1**(1), pp. 899–902. DOI: 10.1007/s12289-008-0241-7.

[26] Alshahrani, H., and Hojjati, M., 2016, "Influence of Double-Diaphragm Vacuum Compaction on Deformation during Forming of Composite Prepregs," J. Sci. Adv. Mater. Devices, pp. 1–5. DOI: 10.1016/j.jsamd.2016.09.003.

[27] ten Thije, R., 2007, "Finite Element Simulations of Laminate Composite Forming Processes," PhD thesis, Universiteit Twente, Netherlands.

[28] ten Thije, R. H. W., and Akkerman, R., 2009, "A Multi-Layer Triangular Membrane Finite Element for the Forming Simulation of Laminated Composites," Compos. Part A Appl. Sci. Manuf., **40**(6–7), pp. 739–753. DOI: 10.1016/j.compositesa.2009.03.004.

Journal of Mechanical Design. Received February 07, 2018;
Accepted manuscript posted June 11, 2019. doi:10.1115/1.4044107

Figure Captions List

Journal of Mechanical Design. Received February 07, 2018;
Accepted manuscript posted June 11, 2019. doi:10.1115/1.4044107

Table Caption List

Journal of Mechanical Design. Received February 07, 2018;
Accepted manuscript posted June 11, 2019. doi:10.1115/1.4044107

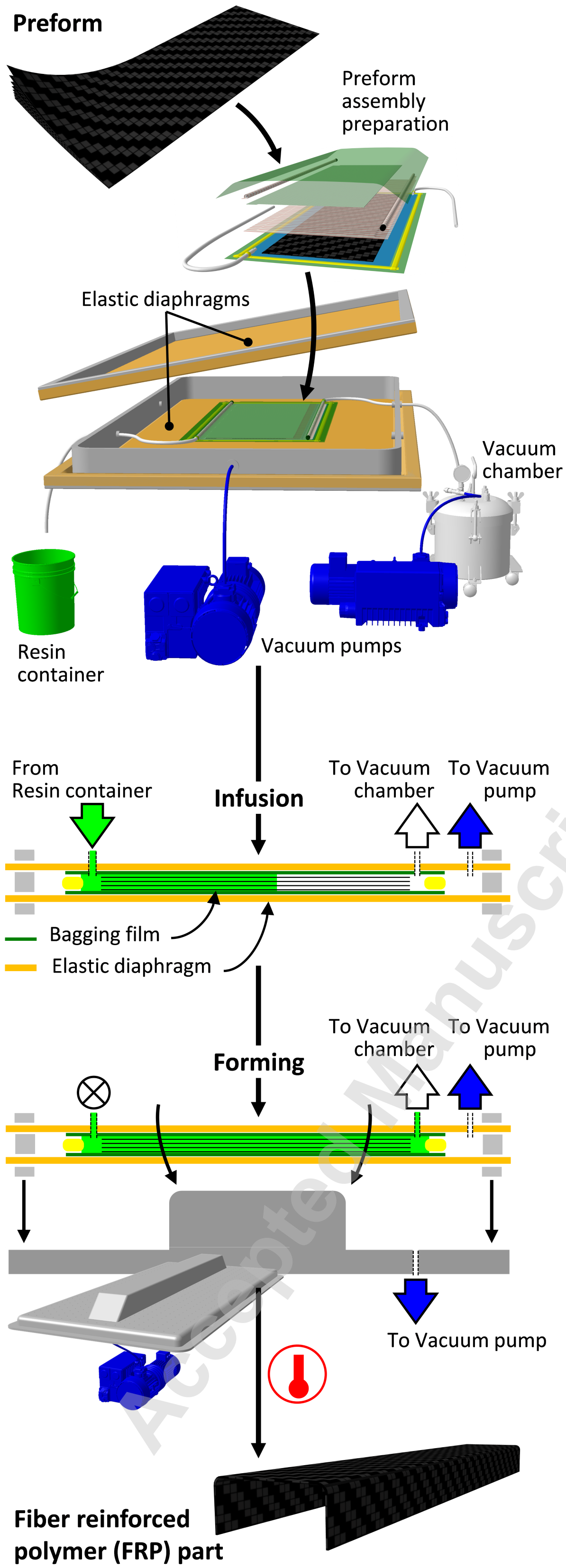

Fig. 1. Flowchart of the in situ forming of a liquid infused preform (ISFLIP) process.

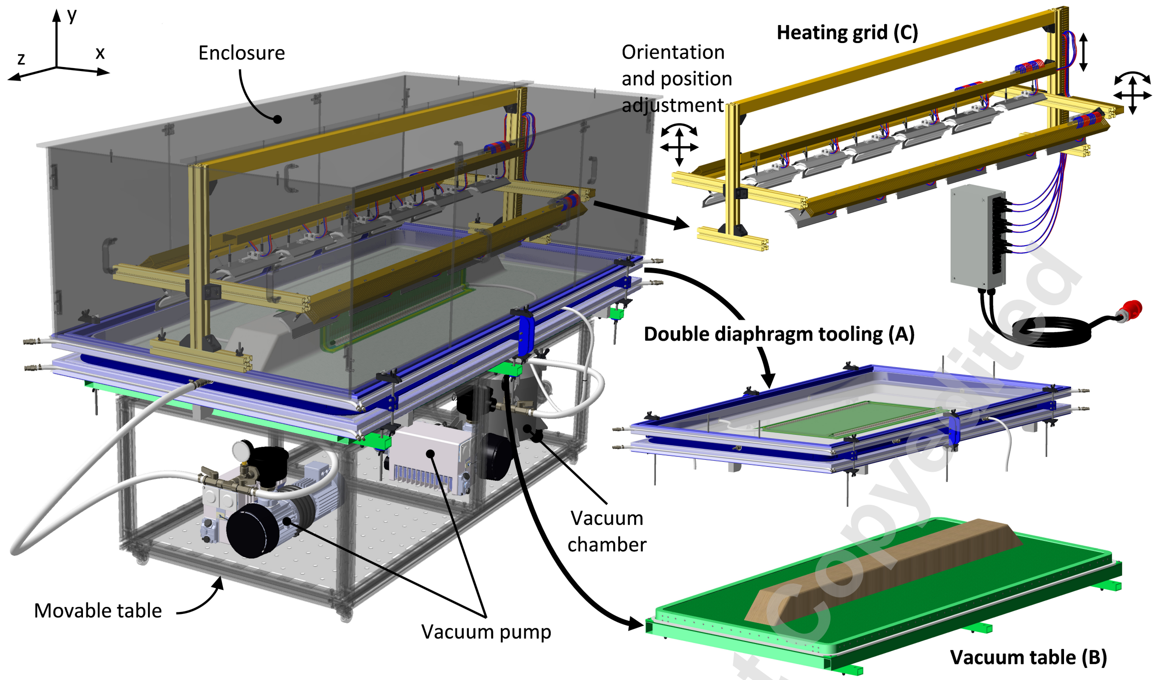

Fig. 2. ISFLIP prototype and the three major subsystems.

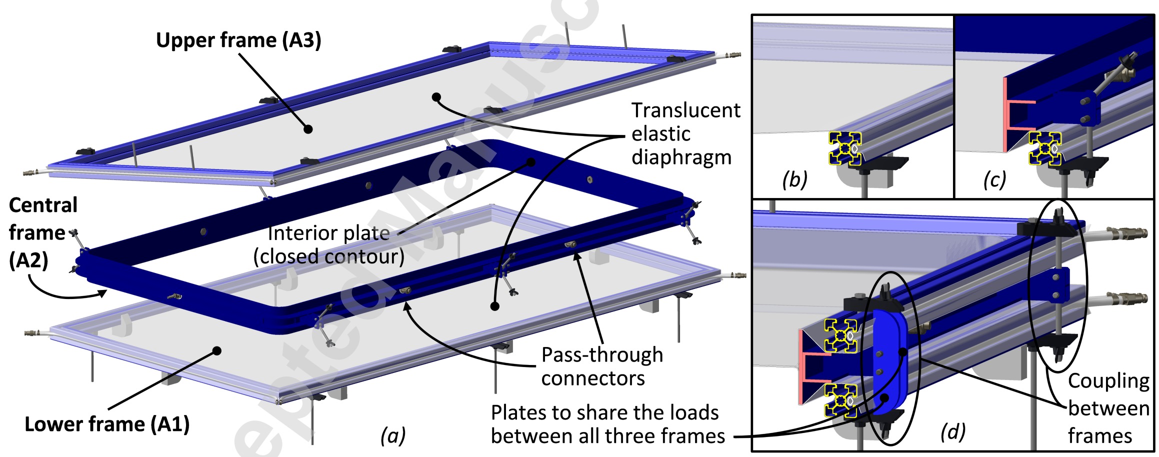

Fig. 3. *(a)* Double diaphragm tooling, *(b)* cross-section view of the lower frame holding a silicone diaphragm, *(c)* cross-section view of the lower frame coupled to the central frame and *(d)* cross-section view of the upper and lower frames coupled to the central frame.

Journal of Mechanical Design. Received February 07, 2018;
Accepted manuscript posted June 11, 2019. doi:10.1115/1.4044107

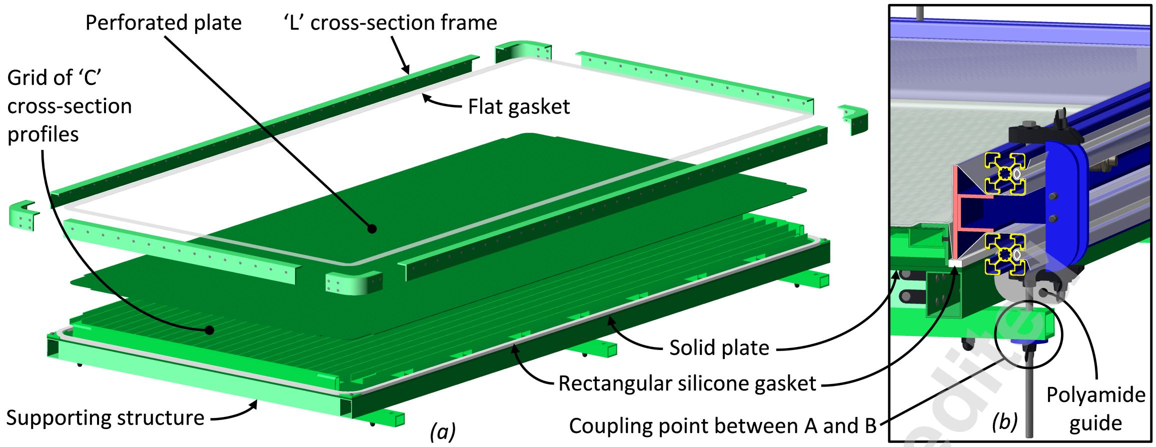

Fig. 4. *(a)* Partially exploded view of the vacuum table (B) and *(b)* cross-section of the double diaphragm tooling (A) and the vacuum table (B) after coupling.

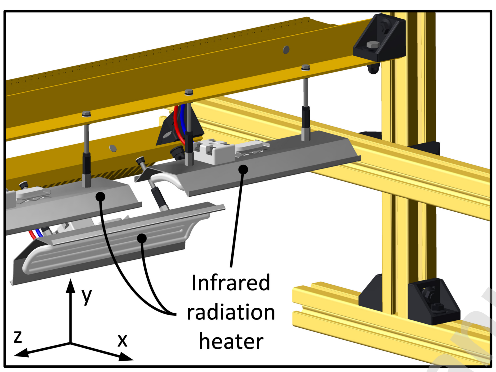

Fig. 5. Close-up view of the infrared heating grid.

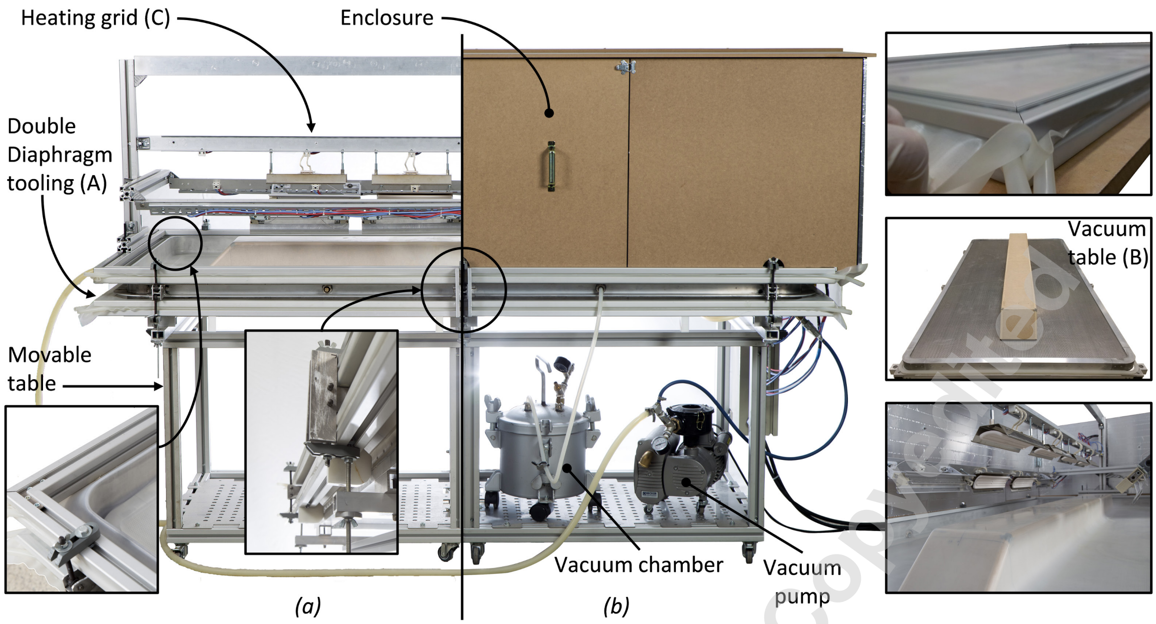

Fig. 6. ISFLIP prototype: *(a)* without enclosure and *(b)* with enclosure.

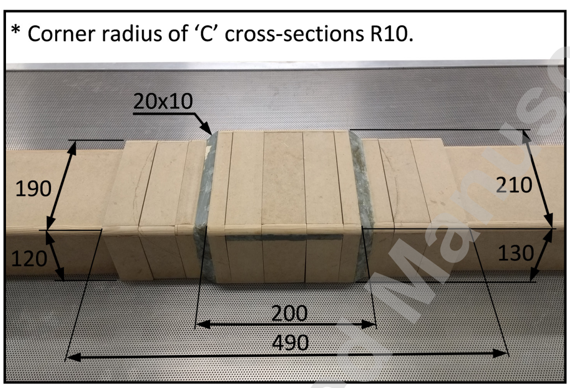

Fig. 7. Mold for manufacturing a 'C' cross-section profile with joggles (built in medium density fiberboard panels).

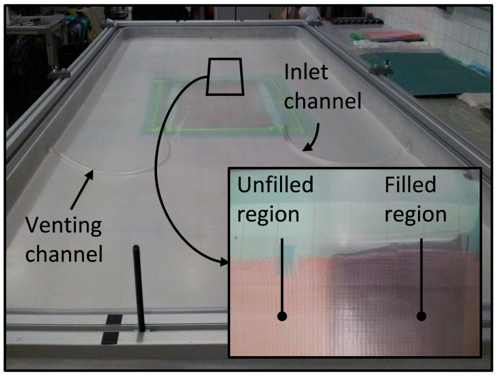

(a)

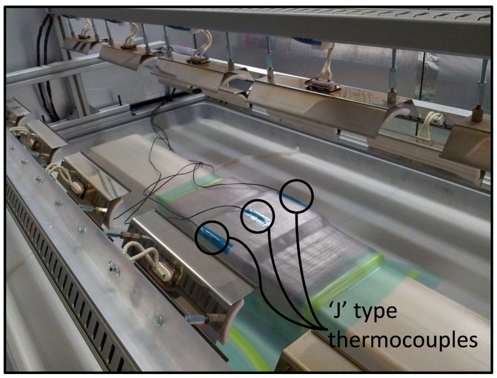

(b)

Fig. 8. Details of the validation test: *(a)* infusion and *(b)* curing stages.

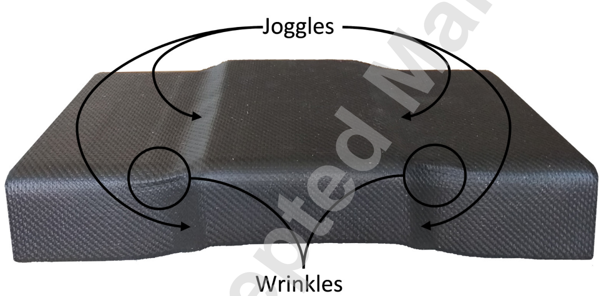

Fig. 9. Manufactured FRP component: 'C' cross-section profile with joggles.